Trans. of the Korean Hydrogen and New Energy Society(2012. 4), Vol. 23, No. 2, pp. 162~172
DOI: http://dx.doi.org/10.7316/KHNES.2012.23.2.162

수소를 연료로 사용한 프리피스톤 리니어 엔진의 수치해석에 관한 연구

왼바흥[1] · 오용일[1] · 임옥택[2†]
[1]울산대학교 기계자동차공학과 대학원 , [2]울산대학교 기계자동차공학부

The Research about Free Piston Linear Engine Fueled with Hydrogen using Numerical Analysis

NGUYEN BA HUNG[1], YONGIL OH[1], OCKTAECK LIM[2†]
[1]Graduate of Mechanical and Automotive Engineering, University of Ulsan, Mugeo-dong, Nam-gu, Ulsan 680-749, Korea
[2]Department of Mechanical and Automotive Engineering, University of Ulsan, 102 Daehak-ro, Nam-gu, Ulsan 680-749, Korea

Abstract >> This paper presents a research about free piston linear engine (FPLE) fueled with hydrogen, in which, the numerical models are built to simulate the operation during the full stroke of the engine. Dynamic model, linear alternator model and thermodynamic model are used as the numerical models to predict piston velocity, in-cylinder pressure and electric power of FPLE. The spark timing and air gap length are changed to provide information for the prediction. Beside, the heat transfer problem is also investigated in the paper. The results of research are divided by two parts, including motoring mode and firing mode. The result of motoring mode showed that there is validation between simulation and experiment for volume and pressure in cylinder. For firing mode, by increasing spark timing, the velocity of piston, peak pressure and electric power also increase respectively. Beside, when increasing air gap length, the electric power increases accordingly while the motion of piston is not symmetric. The effect of heat transfer also observed clearly by reducing of the peak pressure, velocity of piston and electric power.

Key words : Free piston(프리피스톤), Linear engine(리니어 엔진), Hydrogen(수소), Linear generator(리니어 발전기)

Nomenclature

A_B : area of bore
P_a : intake pressure
P_l : pressure in left cylinder
P_r : pressure in right cylinder
F_f : friction force
F_e : electric force
F_{sl} : spring force in the left
F_{sr} : spring force in the right
m : mass
x : displacement of translator
x_0 : initial coordinate of translator
a : acceleration of translator
t : time
P_{cl} : compress pressure in left cylinder
P_{cr} : compress pressure in right cylinder
x_{epl} : the left exhaust port closing coordinate
x_{epr} : the right exhaust port closing coordinate

†Corresponding author : otlim@ulsan.ac.kr
[접수일 : 2012.1.26 수정일 : 2012.4.2 게재확정일 : 2012.4.2]

x_m : the maximum stroke of piston
x_{cl} : position of left piston in compress process
x_{cr} : position of right piston in compress process
p : instantaneous pressure in cylinder
γ : specific heat ratio
V : instantaneous volume in cylinder
Q_c : combustion heat
Q_{in} : heat input
Q_{ht} : heat transfer
χ : mass fraction burned
t_0 : start of combustion
Δt : duration combustion
h : heat transfer coefficient
A_t : heat transfer area
T : instantaneous temperature in cylinder
T_w : wall temperature
P_{el} : expansion pressure in left cylinder
P_{er} : expansion pressure in right cylinder
P_{ecl} : pressure at the end of combustion in left cylinder
P_{ecr} : pressure at the end of combustion in right cylinder
n : polytropic exponent
x_{ecl} : coordinate of left piston at the end of combustion
x_{ecr} : coordinate of right piston at the end of combustion
x_{el} : position of left piston in expansion process
x_{er} : position of right piston in expansion process
M_F : mean magneto motive force
H_c : magnetic field strength
h_m : thickness of permanent magnet
τ : pole pitch
τ_p : width of permanent magnet
x_m : coordinate of survey point in translator axis
x_s : coordinate of survey point in stator axis
x_p : displacement of piston
μ_0 : permeability
g : air gap length
B : magnetic induction density
Φ : flux contained in the coil
N_{coil} : number of turn in the coil
λ : total flux contained in the coil
H : length of coil cutting magnetic line
i : current in the equivalent circuit
ε : voltage generating operation
R_I : internal resistance of coil
R_L : load resistance
L : induction
K : load coefficient
W : average cylinder gas velocity
V_d : displaced volume
V_r : volume at reference state
P_r : pressure at reference state
T_r : temperature at reference state
P_m : motored cylinder pressure
$\overline{s_p}$: average speed of piston

1. Introduction

A free piston linear engine (FPLE) is a crankless internal combustion engine with free motion of piston in cylinder. The engine is the combination of two main components: one is the free piston engine, and another is the linear alternator. In this engine, the motion of piston is determined by the interaction of forces from the combustion chamber gases, rebound device (e.g a spring) and load device (e.g a linear alternator). The advantage of FPLE is a simple structure with a few moving parts, thus it allows to reduce the frictional losses. Unlike the conventional engines with crankshaft mechanism, the FPLE can optimize the combustion process through the variable compression ratios. In other part, the variation of compression ratio in FPLE also allows the engine to operate with multi-fuel. One of fuels used in FPLE is hydrogen which is considered an environmentally friendly fuel and likely will displace fossil fuels in the future. Jakob Fredriksson[1] studied a free piston engine with four kinds of fuel such as diesel, hydrogen, gasoline and natural gas. One of the studied results showed that, the hydrogen case showed a higher efficiency than the gasoline case, although its compression ratio is somewhat lower. In general, the FPLE is classified into three

types including single piston, dual piston and four pistons[2]. The type of single piston has a simple design with high controllability compared to the other free piston engine, however the dynamic balance is not good due to it only has one piston. In case of four piston engine, the perfectly balanced design is the main advantage of this engine, however it also makes the engine complicated. For dual piston engine, the working piston provides the work to drive the compression process in the other cylinder, it allows a simple device with higher power/weight ratio[3]. However, the free motion of dual piston in the cylinder will lead to variation about combustion pressure at each cylinder. Seppo Tikkanen[4] presented experimental results of dual hydraulic free piston engine, which combines a diesel engine and a hydraulic pump into one compact component. The experimental results showed that the combustion pressure variation was about ± 7%, and the variation of combustion pressure at each cycle was from 77 bar to 88 bar.

The paper presents a research about FPLE fueled hydrogen with type of dual piston, in which, free piston engine is combined with a linear alternator, which is used to generate electric power. The research focuses mainly on the numerical analysis of this engine through simulation models. The effects of various spark timing, air gap length and heat transfer on the in-cylinder pressure, piston speed and electric power are investigated in the paper.

2. System Components and Operating Principle

Fig. 1 is the operating model of the FPLE, which includes two main components: free piston engine and linear alternator.

The first component is the free piston engine which contains dual piston or opposed-piston connected by

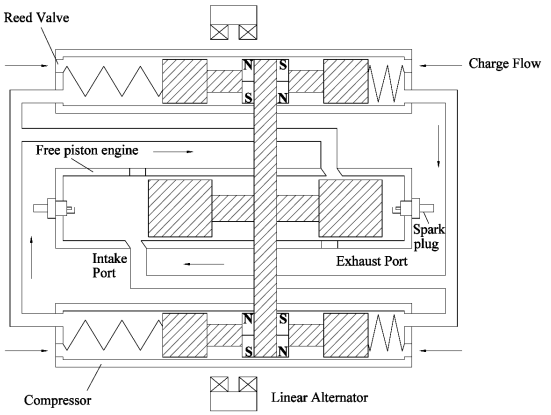

Fig. 1 The operating model of FPLE

connecting rod system. In the engine, the spark plug is arranged at each cylinder head to ignite hydrogen-air mixture. There are two intake ports and one exhaust port around circumference at the bottom of each cylinder. Compressor is arranged at two sides from free piston engine to increase intake pressure to cylinder[5]. Each compressor includes two springs arranged in each cylinder and dual piston which is connected by connecting rod system. Beside, the compressor contains a reed valve to allow intake mixture go into in one way. The second component is the linear alternator with the permanent magnet mounted on the connecting rod as the translator. The back iron made of Silicon steel material and the windings are arranged in the stator.

When the system starts to operate, the linear alternator will operate as the beginning device to drive free piston engine through connecting rod system, it is called motoring mode. After certain frequencies, the combustion process will occur alternatively at each cylinder, forcing connecting rod to move back and forth. The movement of connecting rod will generate the current in the winding due to the magnetic flux linked with winding in stator is changed, and this is called firing mode or generator mode.

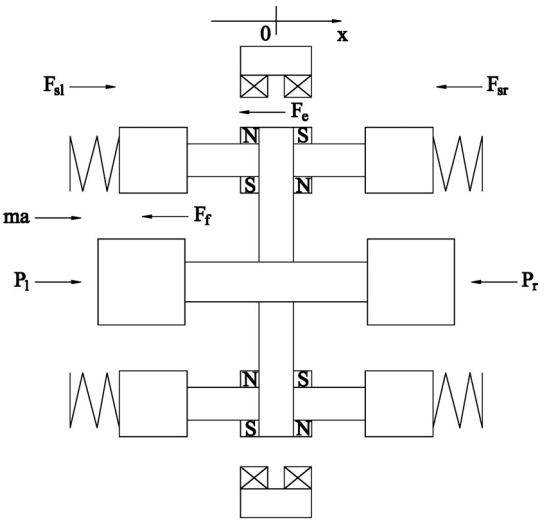

Fig. 2 Free body diagram of FPLE

3. Simulation Model

The objective of this section is to develop a numerical model that describes the operation of FPLE. There are three simulation models used in the analysis including dynamic model, linear alternator model and thermo-dynamic model.

3.1 Dynamic model

The forces applied on the linear engine are expressed through a free body diagram as Fig. 2.

The dynamic model is described by equation that obeys Newton's second law:

$$P_l A_B - P_r A_B - F_f - F_e + F_{sl} - F_{sr} = m\frac{d^2x}{dt^2} = ma \tag{1}$$

The velocity and position of translator can be found by equations:

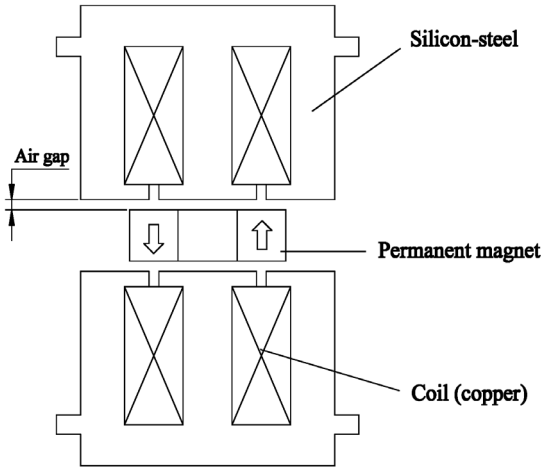

Fig. 3 Schematic of the linear alternator

$$\frac{dx}{dt} = \left(\frac{dx}{dt}\right)_0 + \frac{d^2x}{dt^2}t \tag{2}$$

$$x = x_0 + \frac{dx}{dt}t + \frac{\left(\frac{d^2x}{dt^2}t^2\right)}{2} \tag{3}$$

3.2 Linear alternator model

The schematic of the linear alternator including stator and translator is described in Fig. 3. The air gap is the space between stator and translator. Base on the Fig. 3, the model of a single phase linear alternator with permanent magnet is built as shown in Fig. 4[6].

The permanent magnet which mounted on translator creates a magneto motive force (MMF) in the air gap between the stator and translator. Base on the description in Fig. 4, the MMF can be obtained:

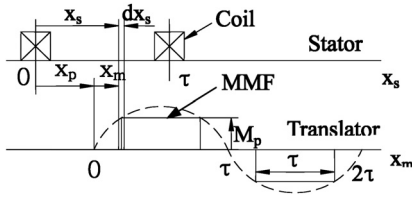

Fig. 4 Model of the linear alternator

$$M_F(x_m)=\begin{cases}0 & 0<x_m<\dfrac{\tau-\tau_p}{2}\\ M_p & \dfrac{\tau-\tau_p}{2}<x_m<\dfrac{\tau+\tau_p}{2}\\ 0 & \dfrac{\tau+\tau_p}{2}<x_m<\dfrac{3\tau-\tau_p}{2}\\ -M_p & \dfrac{3\tau-\tau_p}{2}<x_m<\dfrac{3\tau+\tau_p}{2}\\ 0 & \dfrac{3\tau+\tau_p}{2}<x_m<2\tau\end{cases} \quad (4)$$

Where $M_p = H_c.h_m$

The mean value of the MMF can be defined by the equation as follow[7]:

$$M_F(x_m)=\frac{a_0}{2}+a_1\cos\left(\frac{\pi x_m}{\tau}\right)+b_1\sin\left(\frac{\pi x_m}{\tau}\right) \quad (5)$$

Where

$$a_0=\frac{1}{\tau}\int_0^{2\tau}M_F(x_m)dx_m=0 \quad (6)$$

$$a_1=\frac{1}{\tau}\int_0^{2\tau}M_F(x_m)\cos\left(\frac{\pi x_m}{\tau}\right)dx_m=0 \quad (7)$$

$$b_1=\frac{1}{\tau}\int_0^{2\tau}M_F(x_m)\sin\left(\frac{\pi x_m}{\tau}\right)dx_m =\frac{4}{\pi}M_p\sin\left(\frac{\pi\tau_p}{2\tau}\right) \quad (8)$$

Finally, the mean value of the MMF can be written as below:

$$M_F(x_m)=\frac{4}{\pi}M_p\sin\left(\frac{\pi\tau_p}{2\tau}\right)\sin\left(\frac{\pi x_m}{\tau}\right) \quad (9)$$

The flux density in the air gap is calculated by equation:

$$B(x_m)=\frac{\mu_0}{g}M_F(x_m)=B_m\sin\left(\frac{\pi x_m}{\tau}\right) \quad (10)$$

Where

$$B_m=\frac{\mu_0}{g}\frac{4}{\pi}M_p\sin\left(\frac{\pi\tau_p}{2\tau}\right) \quad (11)$$

The flux contained in the differential element dx_s is calculated by equation:

$$d\phi=B(x_s)dA=B(x_s).H.dx_s \quad (12)$$

Combine the equation (10) with the Fig. 2, the equation (12) is rewritten as follow:

$$d\phi=B_m.H.\sin\left(\frac{\pi(x_s-x_p)}{\tau}\right).dx_s \quad (13)$$

Because the permanent magnet linear alternator operates on the same basic physical principles as conventional rotary alternators, so the voltage generating operation of the alternator is Faraday's Law expressed as[8]:

$$\varepsilon=-\frac{d\lambda}{dt}=-N_{coil}\frac{d\phi}{dt} \quad (14)$$

Combine the equation (13) and the equation (14), the total flux contained in the coil can be derived:

$$\lambda=N_{coil}\int_0^{\tau}B_m.H.\sin\left(\frac{\pi(x_s-x_p)}{\tau}\right)dx_s =\tau.H.N_{coil}.B_m.\frac{2}{\pi}.\cos\left(\frac{\pi x_p}{\tau}\right) \quad (15)$$

The voltage generating operation is also calculated by the equivalent circuit of the linear alternator as follow[8]:

$$\varepsilon = (R_I + R_L).i + L\frac{di}{dt} \tag{16}$$

From the equation (16), the induced current can be easily found:

$$i = \frac{\varepsilon}{R_I + R_L}\left(1 - e^{-\frac{R_I+R_L}{L}t}\right) \tag{17}$$

The electromagnetic force which contained in equation (1) is determined by equation:

$$F_e = i\frac{\partial \lambda}{\partial x_p} \tag{18}$$

Combine the equations (14), (15), (17) and (18), the electromagnetic force can be derived:

$$F_e = \frac{1}{R_I + R_L}\left(1 - e^{-\frac{R_I+R_L}{L}t}\right)H^2.N_{coil}^2.4.B_m^2.\sin^2\left(\frac{\pi x_p}{\tau}\right).\frac{dx_p}{dt}$$

$$= K\left(1 - e^{-\frac{R_I+R_L}{L}t}\right)\sin^2\left(\frac{\pi x_p}{\tau}\right).\frac{dx_p}{dt} \tag{19}$$

Where:

$$K = \frac{1}{R_I + R_L}H^2.N_{coil}^2.4.B_m^2$$

3.3 Thermodynamic model

Thermodynamic model is described by processes such as compression, combustion, expansion and scavenging. In which, the scavenging is assumed as a perfect process.

The compression process is calculated between the time when exhaust port is closed and when the spark occurs. In the analysis, compression process is assumed to obey a polytropic equation. The pressure during compression process is given as follow:

$$P_{cl}(t) = P_a\left(\frac{x_m + x_{epl}}{x_m + x_{cl}(t)}\right)^n \tag{20}$$

$$P_{cr}(t) = P_a\left(\frac{x_m - x_{epr}}{x_m - x_{cr}(t)}\right)^n \tag{21}$$

The combustion process is assumed to occur immediately after the spark occurs, which means that the ignition delay is ignored. The pressure in the combustion process is calculated as follow:

$$\frac{dp}{dt} = -\gamma\frac{p}{V}\frac{dV}{dt} + \frac{\gamma - 1}{V}\left(\frac{dQ_c}{dt}\right) \tag{22}$$

$$\frac{dQ_c}{dt} = \frac{dQ_{in}}{dt} - \frac{dQ_{ht}}{dt} \tag{23}$$

The heat release rate dQ_{in}/dt is calculated when the mass fraction burned is known. The mass fraction burned can be found through the Wiebe function. The Wiebe function is usually used to calculate the mass fraction burned versus crank angle for crankshaft engine. Because the FPLE has no crankshaft, the mass fraction burned is calculated as a function of time

$$\chi = 1 - \exp\left[-a\left(\frac{t - t_0}{\Delta t}\right)^{m+1}\right] \tag{24}$$

Where, a and m are adjustable parameter (according to Heywood[9], a=5, m=2), t0 is the start of com-

bustion, Δt is the total combustion duration.

By differential two sides of the equation (24), the mass fraction burned rate is given

$$\frac{d\chi}{dt} = a\frac{m+1}{\Delta t}\left(\frac{t-t_0}{\Delta t}\right)^m \exp\left[-a\left(\frac{t-t_0}{\Delta t}\right)^{m+1}\right] \quad (25)$$

From equation (25), the heat release rate can be calculated as follow

$$\frac{dQ_{in}}{dt} = a\frac{m+1}{\Delta t}\left(\frac{t-t_0}{\Delta t}\right)^m \exp\left[-a\left(\frac{t-t_0}{\Delta t}\right)^{m+1}\right].Q_{in} \quad (26)$$

The heat transfer rate is calculated by

$$\frac{dQ_{ht}}{dt} = h.A_t.(T-T_w) \quad (27)$$

In the equation (27), the heat transfer coefficient is calculated by

$$h = 3.26.B^{-0.2}.P^{0.8}.T^{-0.55}.W^{0.8} \quad (28)$$

Where

$$W = \left[C_1\overline{S}_p + C_2\frac{V_dT_r}{P_rV_r}(P-P_m)\right] \quad (29)$$

The expansion process is given from the end of combustion process until the exhaust port opens. The process is also assumed to obey a polytropic equation:

$$P_{el}(t) = P_{ecl}\left(\frac{x_m + x_{ecl}}{x_m + x_{el}(t)}\right)^n \quad (30)$$

Table 1 Parameters are used in simulation

Parameters	Value	Unit
Bore	30	mm
Reciprocating mass	0.974	kg
Exhaust port open	20	mm
Maximum stroke	35	mm
Polytropic exponent	1.4	
Intake pressure	1.1	bar
Intake temperature	300	K
Equivalent ratio	0.9	
Combustion duration	1.5	ms
Load coefficient (K)	12.5	N.s/m
The natural length of spring	60	mm
Spring hardness	2.9	N/mm
Frictional coefficient	1.04	
Lower heating value of hydrogen	120	MJ/kg

$$P_{er}(t) = P_{ecr}\left(\frac{x_m - x_{ecr}}{x_m - x_{er}(t)}\right)^n \quad (31)$$

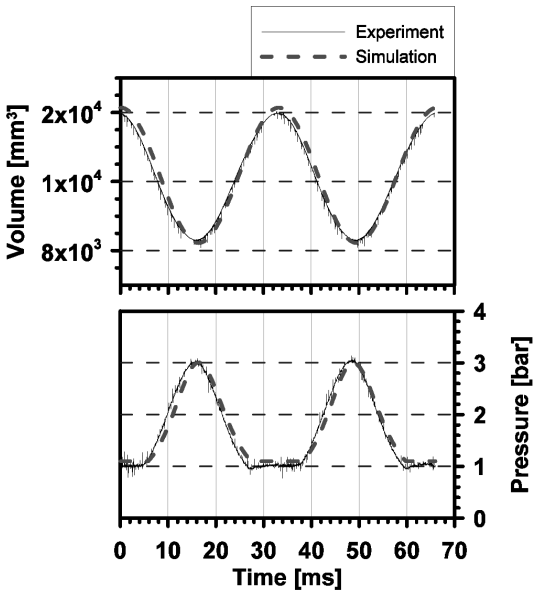

Fig. 5 Volume and pressure versus time

4. Results and Discussion

The models mentioned above ware calculated by a Fortran program based on simulation parameters listed in Table 1. These parameters are chosen base on operated conditions and specifications of actual FPLE.

4.1 Motoring mode

In order to validate simulation process as well as make a base for next steps in the simulation, comparing between simulation and experiment at motoring mode is necessary. Fig. 5 describes the results of volume and pressure in the cylinder versus time at the same condition of intake pressure (Pin=1.1bar) and intake temperature (Tin=300K). The results show that, there is no significant variation between experiment and simulation result.

As mentioned before, the motoring mode would be maintained in FPLE until the combustion process occurs at each cylinder, it's mean that the firing mode was formed immediately after the end of motoring mode. Therefore, the motoring mode plays an important role in simulation at the next mode as well as choice input parameters.

4.2 Firing mode

4.2.1 The effect of spark timing

The spark timing is determined by position of piston before cylinder head that a spark will occur in the combustion chamber. Adjusting spark timing will effect to operation of the engine because it relates directly to combustion process of fuel. Especially, in regard to hydrogen fuel, adjusting spark timing will be sensitive because the burning speed of hydrogen is very high compared with those for other fuels[10].

Fig. 6 describes the piston velocity versus displacement for different spark timing (ignition positions before cylinder head, mm).

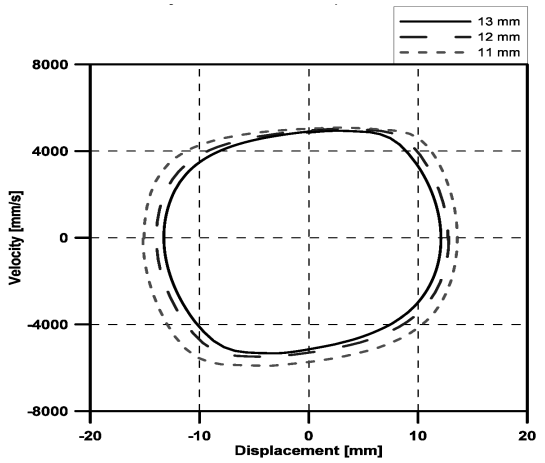

Fig. 6 Piston velocity versus displacement

By increasing spark timing or decreasing ignition positions before cylinder head from 13 mm to 11 mm, the maximum velocity of piston is increase respectively. This is because the heat release occurs after TDC, (according to the Wiebe function) while spark timing occurs before TDC. Therefore, when increasing spark timing, the heat release converted to expansion work is increased and it makes the velocity of piston increasing.

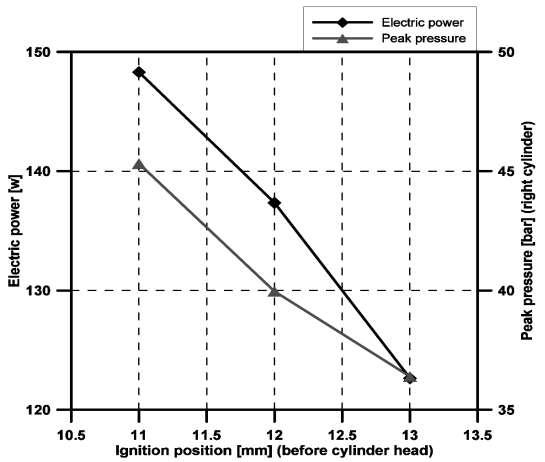

Fig. 7 Electric power and peak pressure versus ignition position

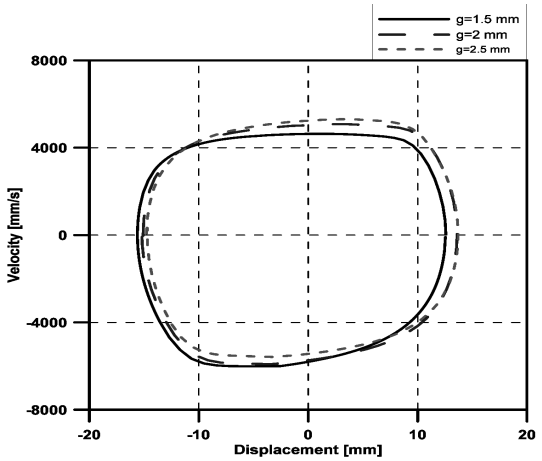

Fig. 8 Piston velocity versus displacement

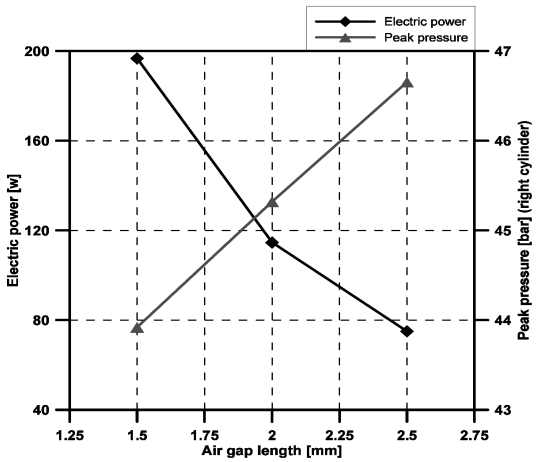

Fig. 9 Electric power and peak pressure versus air gap length

As a result, the maximum stroke as well as compression ratio of FPLE is increased. The variation of the maximum velocity at the forward and backward stroke can be also observed. This is because the pressure drop at the end of expansion stroke in right cylinder is higher than that in left cylinder due to the increase of spark timing. At forward stroke, the maximum velocity of piston corresponds to position that exhaust port in left cylinder starts to open. For backward stroke, the maximum velocity of piston corresponds to position that exhaust port in right cylinder starts to open. Due to the opening of exhaust port, the pressure difference at each cylinder is decreased, and it lead to the maximum velocity of piston will decrease immediately after obtain maximum value.

Fig. 7 shows a plot of electric power and peak pressure versus different ignition positions. When the ignition position before cylinder head is decreased from 13 mm to 11 mm, the electric power and peak pressure increase respectively. This can be due to the increasing of piston velocity as shown in Fig. 6.

4.2.2 The effect of air gap length

Fig. 8 describes the effect of air gap length on the velocity of piston.

It can be seen that, the variation of maximum velocity in the forward and backward stroke is increased when the air gap length is decreased, especially at the air gap length equal 1.5 mm. This is because when decreasing air gap length from 2.5 mm to 1.5 mm, the electric force increases accordingly. As the result, the velocity of piston and displacement in positive direction at forward stroke will decrease. This lead to heat release in the expansion process of right cylinder is larger, therefore the velocity of piston in backward stroke is

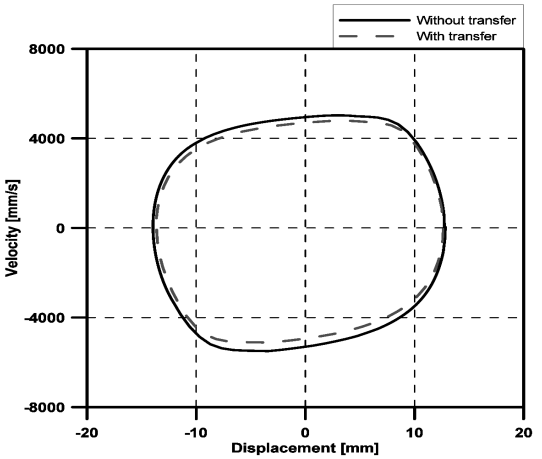

Fig. 10 Piston velocity versus displacement

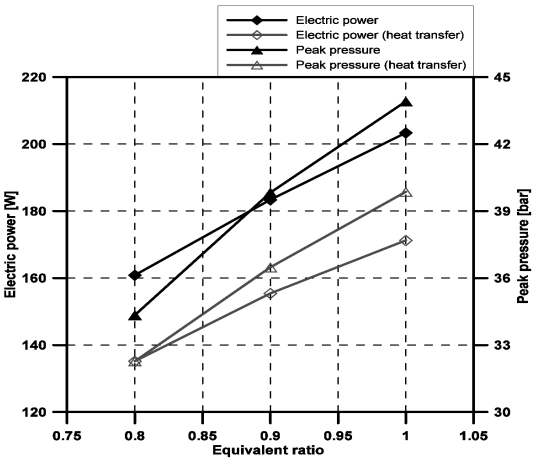

Fig. 11 Electric power and peak pressure versus equivalent ratio

increased.

Fig. 9 illustrates the effect of air gap length on electric power and peak pressure in right cylinder. When the air gap length is increased, the electric power decreases respectively due to the decrease of electric force. However, the peak pressure in right cylinder increases when the air gap length is increased. This is due to the displacement of piston in positive direction increases as shown in Fig. 8.

4.2.3 The effect of heat transfer

The effect of heat transfer on the velocity of piston is described in Fig. 10.

It can be found that, the maximum velocity of piston is decreased when the heat transfer problem is added in the simulation. This is simply because heat release lead to decreasing of in-cylinder pressure. As the result, the maximum velocity is decreased. Fig. 11 illustrates the effect of heat transfer on electric power and peak pressure at different equivalent ratios. By increasing the equivalent ratio, the electric power and peak pressure is increased for both without transfer and with transfer. Comparing between heat transfer and without transfer shows that, both electric power and peak pressure in case of heat transfer are smaller than those of without heat transfer. E.F Shoukry[11] found that by eliminating the heat transfer, the in-cylinder pressure and the velocity of piston were also increase. He also found that the heat transfer was about 22 to 26% of the total power.

5. Conclusion

This paper presented the simulation of FPLE through the combination of three models, dynamic model, linear alternator model and thermodynamic model. The simulation results shows that

1) By increasing spark timing or decreasing ignition position which is distance between piston and cylinder head, the maximum velocity, electric power and peak pressure increase accordingly.
2) When the air gap length increases, the electric power is decreased. Beside, by increasing the air gap length, the velocity of piston has the trend to balance better.
3) The maximum velocity, electric power and peak pressure is decreased when the heat transfer is calculated.

Acknowledgement

This work was supported by the development program of local science park funded by the ULSAN Metropolitan City and the MEST (Ministry of Education, Science and Technology)

References

1. J. Fredriksson and I. Denbratt, Simulation of a Two-Stroke Free Piston Engine, SAE, 2004,

2004-01-1871.
2. Q.F. Li, J. Xiao, and Z. Huang, Simulation of a Two-Stroke Free-Piston Engine for Electrical Power Generation, Energy & Fuels, 2008.
3. R. Mikalsen, A.P. Roskilly, A review of free-piston engine history and applications, Applied Thermal Engineering, Vol. 27, 2007.
4. S. Tikkanen, M. Lammila, M. Herranen and M. Vilenius, First Cycles of the Dual Hydraulic Free Piston Engine, SAE, 2000, 2000-01-2546.
5. Yongil oh, Gangchul Kim and Ocktaeck Lim, "A Study of Design and Dynamic Characteristics of Compact Linear Engine for Portable Powerpack", 2011, KHNES paper, Vol. 22, 4, pp. 512-519.
6. Z. Deng, I. Boldea, and S.A. Nasar, Fields in Permanent Magnet Linear Synchronous Machines, IEEE Transactions on Magnetic, Vol. Mag-22, 1986.
7. J. Wang, D. Howe, A linear permanent magnet generator for a free-piston energy converter, IEEE, 2005.
8. W. Cawthorne, Optimization of a Brushless Permanent Magnet Linear Alternator for Use with a Linear Internal Combustion Engine, Thesis, West Virginia University, 1999.
9. J.B. Heywood, Internal Combustion Engine Fundamentals, McGraw-Hill Book Company, New York, USA, 1988.
10. T. Wallner, H.K. Ng, R.W. Peters, The effects of blending hydrogen with methane on engine operation, efficiency, and emissions, SAE, 2007, 2007-01-0474.
11. E.F Shoukry, Numerical simulation for parametric study of a two-stroke compression ignition direct injection linear engine, PhD thesis, West Virginia University, 2003.